Supplementary Material (ESI) for Soft Matter

Interfacial Instabilities in a Microfluidic Hele-Shaw Cell: Supplemental

Michinao Hashimoto[1], Piotr Garstecki[2]*, Howard A. Stone[3] and George M. Whitesides[1]*

[1]*Department of Chemistry and Chemical Biology, Harvard University*

12 Oxford St., Cambridge, MA, U.S.A.

[2] *Institute of Physical Chemistry, Polish Academy of Sciences,*

Kasprzaka 44/52, 01-224 Warsaw, Poland

[3] *School of Engineering and Applied Sciences, Harvard University*

29 Oxford St., Cambridge, MA, U.S.A.

Journal: Soft Matter

Email: (GMW) gwhitesides@gmwgroup.harvard.edu; (PG) garst@ichf.edu.pl

Results and Discussion

Structure of the "Fishbone" Pattern. The structure of these patterns could, to some extent, be modulated through changes in the shape of the HSC. Figure S2 shows three examples. In Figure S2a, the outlet channel progressively and gradually increased in width as the droplets traveled downstream. Because the field of flow was not as diverging as that in a rectangular cell, the droplets did not stretch when they enter the cell. The channels illustrated in Figures S2b and S2c had two outlets and a curved shape. The flow of the continuous fluid stretched the droplets into extremely elongated shapes (the aspect ratio – the ratio of width to length – was on the order of 100). These highly elongated droplets underwent a capillary instability and broke into a number of small droplets. Figure S2d and S2e illustrates the pattern formed in the HSC with an entrance of droplets shifted to the side from the center. The shear stress created by higher rates of flow (Figure S2e) forced the droplets to break up near the entrance, producing two sizes of fragments of droplets.

Emergence of the "Corn" Pattern. Figure S3a shows the upper limit of the "fishbone" regime; we observed the appearance of 'nodes' on stretched droplets. As we increased the rate of flow of the continuous phase, stretched droplets started to break more rapidly than at lower rates of flow. They formed perplexingly regular patterns, which we called "corn" for the visual similarity to an ear of corn (Figure S3b and S3c).

Development of SDI in Channels with Various Shapes. In order to study the development of SDI, we designed not only a straight outlet channel but also an outlet

channel with a thinner section (neck), and a curved outlet channel. Figure S4a and S4b display SDI in a regular, rectangular HSC. Figure S4b is a snapshot of a region where SDI occurred. The droplets traveled from the top to the bottom; the image thus displays the stepwise development of tails via SDI. Figure S4c and S4d display droplets traveling in a rectangular channel with a neck. The rate of flow in the neck was higher than in the wide channel, and thus the emergence and development of tails were accelerated in the neck. Figure S4e and S4f display the SDI occurring on stretched droplets that traveled in an S-shaped outlet channel. The onset of the growth of tails started earlier at the outer side of the curve than at the inner side of the curve; droplets experienced higher shear stress at the outside of the curve due to higher rates of flow.

Effects of Surfactants on the Interface of droplets and continuous phase.

Surfactants lower interfacial tension between immiscible liquids and prevent coalescence of droplets, and also change the affinity of liquid phases for solid surfaces (i.e. they change the contact angle). In the current experiments, we added surfactants to both the continuous and dispersed phases. To study the effect of each surfactant on the affinity properties of both liquids, we measured contact angles of aqueous droplets on the hydrophobic surface of PDMS in a bath of hexadecane.

The setting of the experiment appears in Figure S5a. We placed a droplet on a flat PDMS surface immersed in hexadecane. We made sure that the surface of PDMS was hydrophobic by incubating it in a 120 °C oven for 24 hours; the condition of the surface was, we believe, the same as that in the experiments in the HSC. Figure S5b-i illustrates

the change in the contact angle of aqueous droplets with respect to the concentration of Tween 20 in aqueous droplets. At low concentrations of Span 80 (either 0 % or 0.3 % by weight), the contact angles of aqueous droplets did not vary significantly, and remained greater than 90° even though the concentration of Tween 20 is extremely high (10 % by weight, a value one thousand times greater than its critical micelle concentration). We note that the value of the contact angles critically depended on the concentration of Span 80 in the continuous phase. Figure S5b-ii shows the change in the contact angles as a function of the concentration of Span 80, with the concentration of Tween 20 held constant. When an aqueous droplet did not contain Tween 20, contact angles almost remained the same regardless of the concentrations of Span 80. We observed significant dependence of the contact angle on the concentration of Span 80 *only* when the aqueous droplet contained sufficiently high concentrations of Tween 20 (2 % and 10 % by weight). We observed contact angles less than 90° for the aqueous droplets on the PDMS surface only when both aqueous droplets and hexadecane contained high concentrations of surfactants (Tween 20; 2 – 10 % by weight, and Span 80; 3 % by weight). These observations suggest that the aqueous droplets had the highest affinity to the hydrophobic surface of PDMS only when both droplets and continuous phase contains sufficiently high concentration of surfactants.

Effect of co-surfactants. Figure S7 reproduces the series of micrographs showing the variation of the concentrations of these co-surfactants. The addition of ethanol and glycerol showed general trends of the decrease in the interfacial tension; the size of droplets decreased as the concentration of additives increased, but we did not observe significant effects on interfacial instabilities. Unlike amphiphatic surfactant molecules

discussed in the manuscript, these small molecules did not have significant influences on the behaviors of aqueous droplets.

Table S1 summarizes our observations of the behaviors of aqueous droplets with different surfactants and additives and with different concentrations. We initially suspected that the behavior of the droplets did not change significantly by the concentration of surfactants above critical micelle concentration (CMC). In our current system, however, the behavior of the system significantly varied by the concentration of surfactants, regardless if the concentration was above or below CMC. For example, the stretch of droplets took place only when the concentration of Tween 20 was over 100 times greater than its CMC value (0.01 % by weight). Below that concentration, regardless if it was above or below the CMC, droplets remained circular shapes. On the other hand, droplets containing CTAB went through the series of instabilities when the concentration of CTAB was below its CMC (0.1 % by weight). We cannot provide plausible explanations for the behavior of the system at this point since two characteristics of the system made it difficult to predict the behavior of the system based on the values of CMC of surfactants: (1) the system contained two surfactants, Span 80 and co-surfactants that competed for the same interface, and (2) the extensional flows along the interface constantly redistributed the position of surfactants, and changed the concentration of the surfactant on the surface.

Conclusions

Study of Complex Systems via "Synthetic" Approach. As it is the *interaction among* droplets, not just the properties of individual droplets, that led to the formation of patterns, the experimental system that we presented here provided a testbed for studies of complexity or dynamic pattern formation. The study of the current system is an example of a synthetic—as opposed to a reductionist—approaches in which we create a large number of identical components (i.e. droplets); we study collective behaviors of components that results from their interactions. This collection of droplets exhibits unexpected properties that we regard as emergent because the behaviors (i.e. formation of patterns) that we observe cannot be attributed solely to the properties of the individual droplets. An advantage of this "synthetic" complex system is that, although the system exhibits complex behaviors, it is still *simple* in that experimentally accessible parameters such as rates of flows and concentration of surfactants determine the type (and the strength) of the interactions. The construction of such *simple* complex systems builds on the phenomenological knowledge of the dynamics of systems of interacting components. We believe the understanding that we gain through this types of synthetic approach will eventually make it possible to understand more complicated experimental complex systems that we cannot yet analyze with currently established principles.

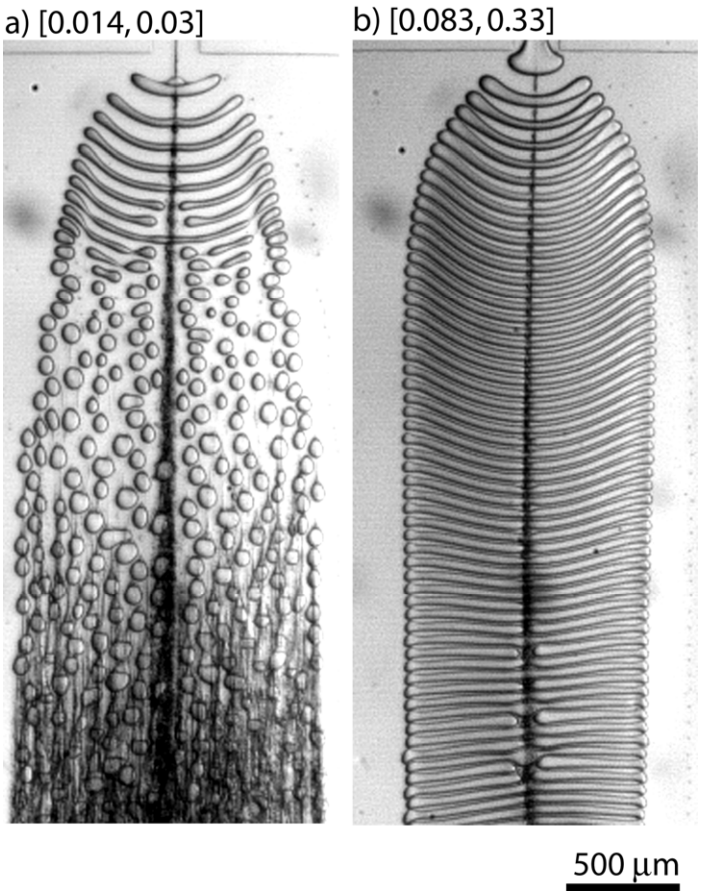

Figure S1. Optical micrographs (top view) of the outlet channels (w_{out} = 2mm). The set of fluids was (water, Tween 20, 2%; hexadecane, Span 80, 3%). **a)** *Rain*. Droplets broke up via capillary instability. The streaks in the bottom part of the figure were liquid films on the top and bottom walls (shear driven instability; SDI). **b)** *Fishbone*. The stretched droplets exhibited greater stability to pulling of the liquid sheets at the walls. The central streak reflected the small droplets formed by the SDI (see Figure 2); the SDI occured to circular droplets in the orifice, before droplets entered the HSC and stretched.

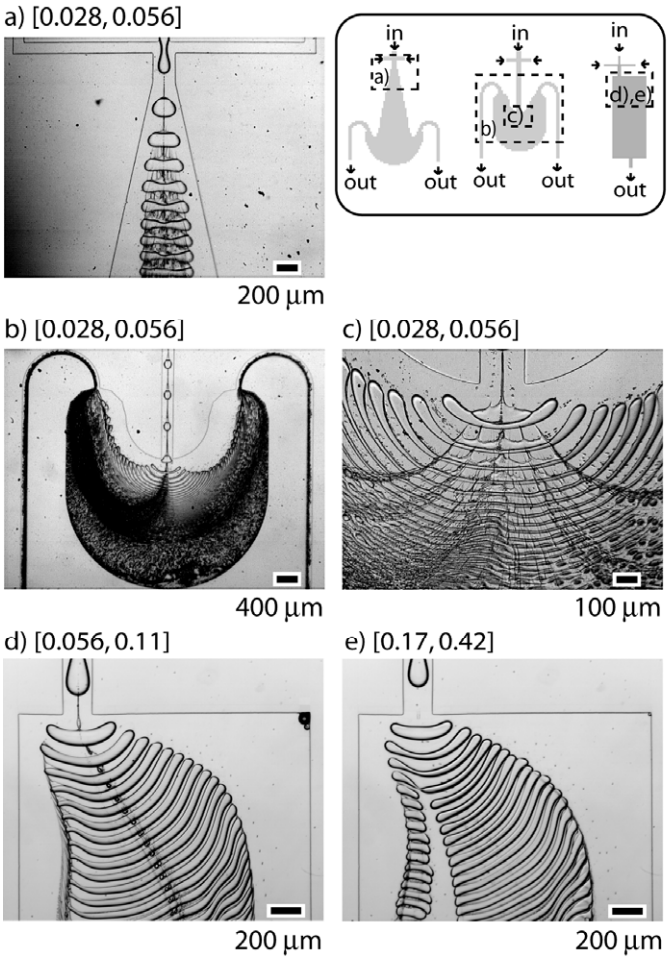

Figure S2. Optical micrographs of stretched droplets in channels with different shapes. The set of fluids was (water, Tween 20, 2 %; hexadecane, Span 80, 3 %). **a)** Weakly diverging flow field (V-outline); the elongation of droplets did not occur in this shape of the cell. **b)** and **c)** Highly diverging flow field (U-outline); droplets entering the channel stretched to both sides until they reached the thickness at with they spontaneously broke up via a capillary instability. **d)** and **e)** Asymmetric flow field; at low rates of flows, droplets stretched similarly to the symmetric, rectangular HSC. At high rates of flows, additional shear stresses drove droplets to break up asymmetrically.

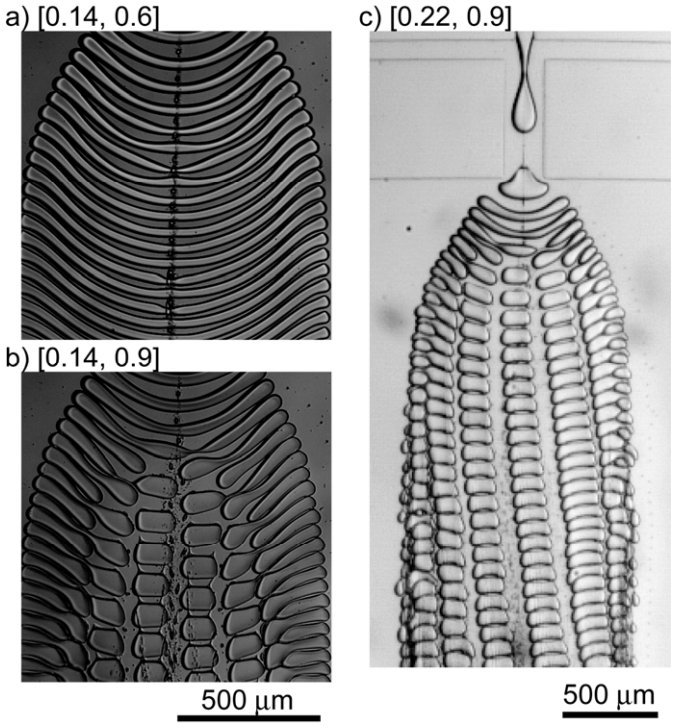

Figure S3. Optical micrographs (top view) of the patterns of droplets formed at high rates of flows (w_{out} = 2 mm). The set of fluids was (water, Tween 20, 2 %; hexadecane, Span 80, 3 %). **a)** Emergence of nodes on elongated droplets, **b)** break-up of elongated droplets at the nodes, and **c)** formation of "*corn*" pattern.

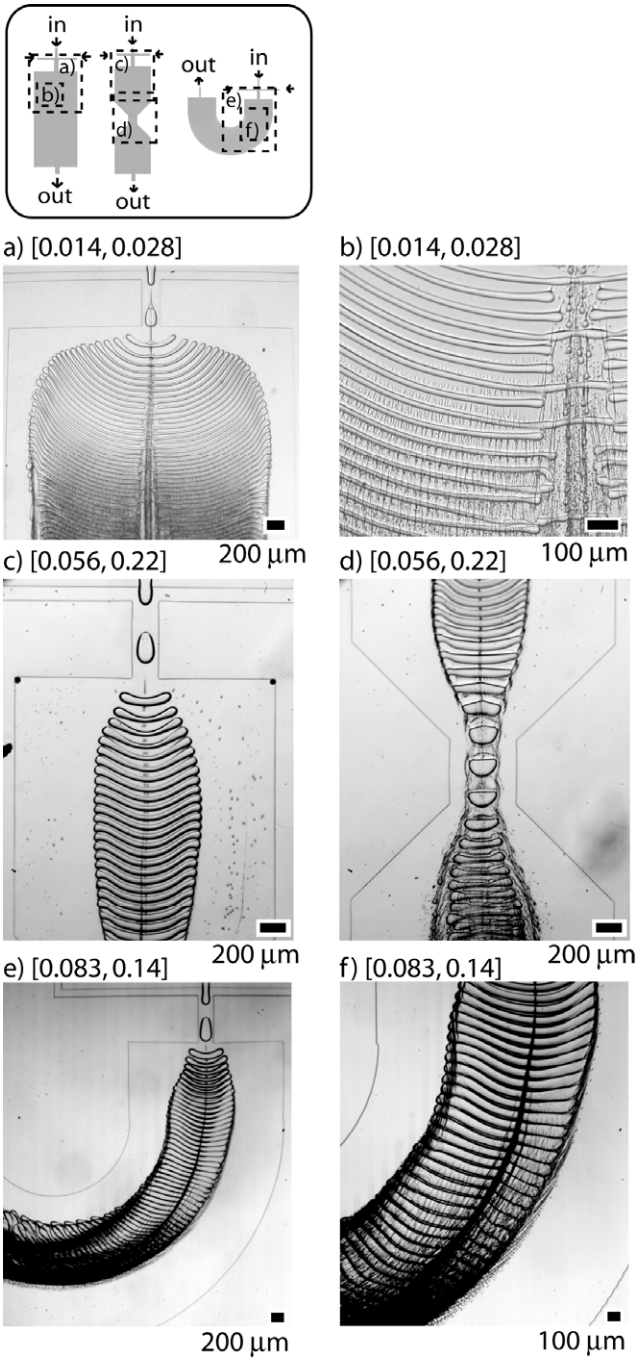

Figure S4. Shear-driven instability (SDI) in **a) – b)** a straight channel, **c) – d)** a straight channel with a neck, and **e) – f)** a curved channel. The set of fluids was (water, Tween 20, 2 %; hexadecane, Span 80, 3 %). **a)** The darker region in the bottom of the image reflected tails that developed from stretched droplets through the SDI. **b)** A magnified image of the tails. The direction of the flow was from the top to the bottom in the image;

the series of the elongated droplets in the micrograph, from top to bottom, displayed the time evolution of the tails from the droplets. **c) – d)** Droplets flowing through a narrow neck developed tails much faster than those flowing in a wide HSC. The increase in the rates of flows accelerated the evolution of SDI in the neck. **e) – f)** Droplets flowing in a curved path. SDI evolved faster in the outer region of the curve than in the inner region of the curve due to higher rates of flows.

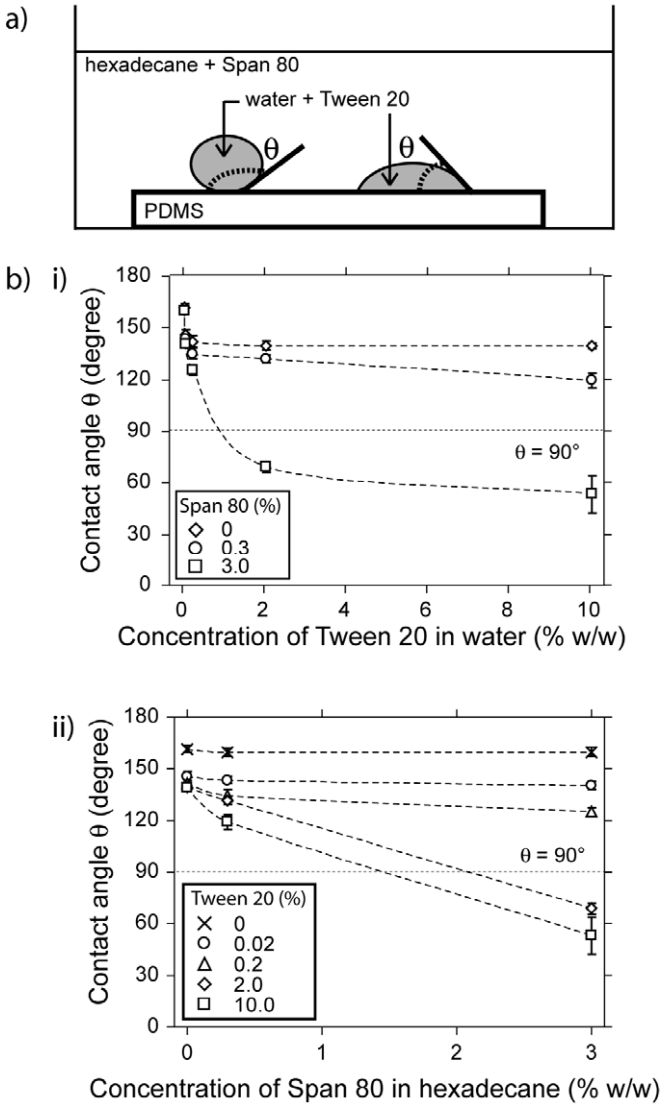

Figure S5. Variation of contact angles with changes in the concentration of surfactants. **a)** Schematic illustration of the measured contact angle (θ). An aqueous droplet was placed on a flat surface of hydrophobic PDMS immersed in hexadecane. The aqueous droplet contained Tween 20, and the hexadecane contained Span 80. **b)** Plots of the contact angle (θ) with respect to the concentration of surfactants: i) concentration of Tween 20 in aqueous phase, and ii) concentration of Span 80 in hexadecane.

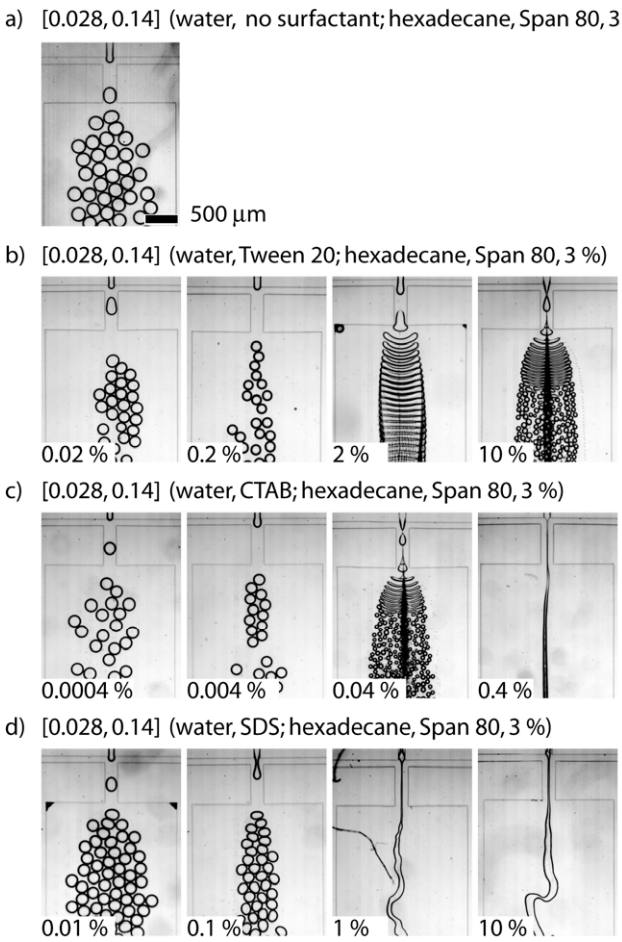

Figure S6. Variations in flow patterns due to surfactants added to the dispersed phase. We used three different surfactants: **a)** Tween 20, **b)** cetyl trimethylammonium bromide (CTAB), and **c)** sodium dodecyl sulfate (SDS). We varied the concentration of each surfactant; the concentration of the surfactant is shown on the left bottom corner of each image. The continuous phase was hexadecane with Span 80 (3 % by weight).

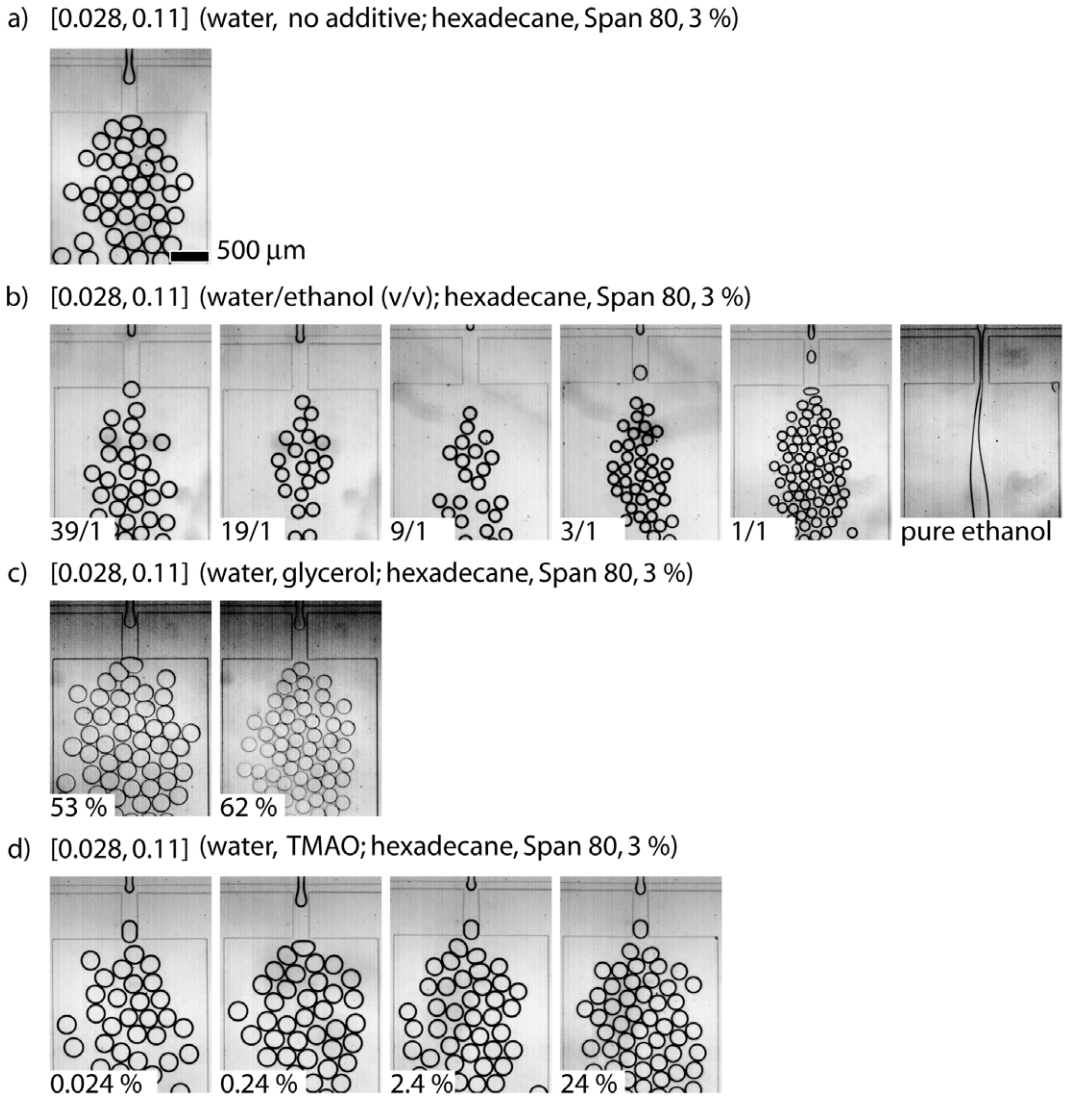

Figure S7. Variations in flow patterns by small molecules added to the dispersed phase. We tested three different small molecules as co-surfactants: **a)** ethanol, **b)** glycerol, and **c)** trimethylamine-N-oxide (TMAO). We varied the concentration of each additive; the concentration of the additive is shown on the left bottom corner of each image. The continuous phase was hexadecane with Span 80 (3 % by weight). For all three additives, we did not observe significant changes in interfacial tension that caused a series of instabilities of droplets.

Table S1. Variation of the type and concentration of additives and the observed patterns of droplets

HD [a] Span 80 (%, w/w)	H_2O Tween 20 (% w/w)	CTAB [a] (%, w/w)	SDS [a] (%, w/w)	ethanol (%, v/v)	glycerol (% w/w)	TMAO [a] (%, w/w)	observation [b]
0	0						coalescence
0	2						coalescence
3	0						circular
3	0.02						circular
3	0.2						circular
3	2						instability
3	10						instability
3		0.0004					circular
3		0.004					circular
3		0.04					instability
3		0.4					no break-up
3			0.01				circular
3			0.1				circular
3			1				no break-up
3			10				no break-up
3				0			circular
3				2.5			circular
3				5			circular
3				10			circular
3				25			circular
3				50			circular
3				100			no break-up
3					53		circular
3					62		circular
3						0.024	circular
3						0.24	circular
3						2.4	circular
3						24	circular

[a] The abbreviations are HD for hexadecane, CTAB for cetyltrimethylammonium bromide, SDS for sodium dodecyl sulfate, and TMAO for trimethylamine N-oxide.

[b] The pattern of observations corresponded to those defined in Figure 7. *Coalescence*: droplets coalesced when they collided with other droplets at the HSC. *Circular*: formed droplets adopted circular shape and remained the circular shape as they flowed to the downstream. *Instability*: droplets stretched in the outlet channel, and underwent a series

of instabilities (i.e. rain, fishbone, corn and SDI). *No break-up*: droplets did not form in the FF generator because the dispersed phase wetted the device.

[c] The rates of flows at which we observed the patterns were [0.028, 0.11] for the series of Tween 20, CTAB, and SDS, and [0.028, 0.14] for the series of ethanol, glycerol and TMAO, where [Q_d (μL/s), Q_c (μL/s)] denoted the rates of flows of the dispersed phase (Q_d) and the continuous phase (Q_c), respectively.